Seismically Induced Overturning of Objects and Filtering Effects of Buildings

David Franke[1], Nelson Lam[2], Emad Gad[3], and Adrian Chandler[4]

1. Visiting Scholar, Department of Civil and Environmental Engineering, University of Melbourne, 3010, Australia
2. Department of Civil and Environmental Engineering, University of Melbourne, 3010, Australia, email: n.lam@civenv.unimelb.edu.au
3. Department of Civil and Environmental Engineering, University of Melbourne, 3010, Australia
4. Centre for Earthquake Engineering Research (CEER), Department of Civil Engineering, University of Hong Kong, Hong Kong SAR, China

ABSTRACT: *The seismic performance of unrestrained objects is critically dependent on the displacement demand behaviour of the building floor. The risk of an object overturning can be estimated from the dual independent criteria of object width and height, as opposed to the usual single criterion of the object aspect ratio (or slenderness ratio) based on static analysis. An object is at risk from overturning if the displacement demand of the floor exceeds one-third of the width of the object. According to floor amplification clauses in earthquake codes of practice, the filtering effects of a building amplify ground motions up its height. However, the building may also behave as an isolation medium, which attenuates the transmitted motions. These two perceptions seem contradictory. This paper aims to resolve this significant dilemma and hence contribute to improving the fundamental understanding of the dynamical processes of damage to building contents. Floor spectra of buildings, as presented in the paper, demonstrate both amplification and isolation actions.*

Keywords: Non-structural components; Building contents; Overturning; Rocking; Displacement floor response spectra

1. Introduction

Damage to non-structural components and contents in a building often constitutes a high proportion of the total damage bill of a major earthquake event. Seismically induced damage to non-structural building components in a building has attracted worldwide research attention in recent years (e.g. [1,2] as latter published in this journal). Major contemporary earthquake codes of practice have incorporated provisions for adequately securing utility components (i.e. mechanical and electrical installations) and architectural components (e.g. building facades and partitions) to the building structure (e.g. in [3-7]).

However, the seismic performance of building contents, which include furniture items, is beyond the scope of building design codes and regulations despite the implications regarding their performance behaviour. For example, the overturning of storage racks, including tall book shelves, could hinder the safe egress of occupants from the confines of a building following an earthquake tremor. The situation has potential life-safety implications if fire is triggered by the tremor, and can be aggravated by black-outs or the spillage of hazardous substances in the moment of panic. Notwithstanding these, overturning of building contents could result in major disruptions to the continuous functioning of facilities and consequently compromise businesses in a significant way. Figure (1) depicts the possible impact of overturning furniture items in a typical office.

The above-described risks could be mitigated by regulatory measures to control the disposition of furniture and storage items throughout the service

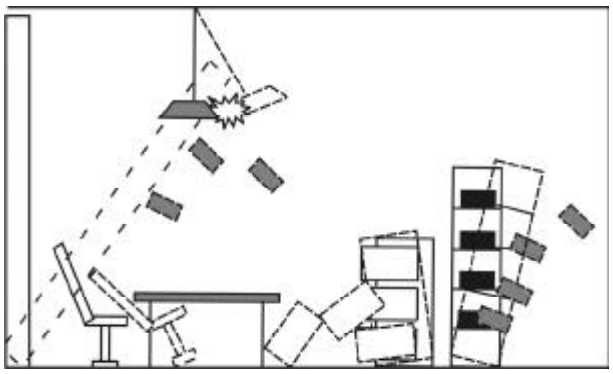

Figure 1. Disruption to an office by overturning of furniture items.

life of the building. Stringent regulations related to occupational health and workplace safety in the developed world are usually implemented by the regular inspection of buildings during their service-life. One of the key safety issues to address in such inspections is ensuring safe egress of the building occupants in the event of a fire. Obviously, the threat from a potential fire in a building seems more imminent, and has been receiving more attention, than that from the infrequent occurrence of an earthquake. This is because fires are reported daily in all major cities, unlike earthquakes. Building fire statistics collected in Europe show that the average annual ignition frequency of a building is in the order of 1 in 10^{-5} to 10^{-6} per metre square of floor space [8]. Thus, an office space of $1000m^2$ is estimated to have a chance of 1 in 100 to 1 in 1000 of sustaining a fire. Interestingly, this probability of occurrence is comparable to that of the 500-year return period design earthquake (i.e. annual occurrence frequency of 1 in 500). It is noted, however, that the risk of a premise on fire is dependent on effective preventive measures that are in place, unlike the occurrence of an earthquake.

The social and economic impact of seismically induced disruptions is compounded by their simultaneous occurrence in a large number of facilities in a short period of time, which is in contrast to an average building fire in a city. It is the opinion of the authors that the potential risks of a building subject to an earthquake should deserve at least as much attention as the fire risk in building safety regulations (as distinct from building design regulations). Such attention is justified in regions of low and moderate seismicity where the notional design peak ground acceleration is only in the order of 0.1*g*. It is noted that contemporary earthquake codes of practice (e.g. Draft [6]) stipulate a ground-to-roof acceleration amplification factor of 3, citing results from analytical investigations based on estimated peak accelerations on the building floor [9]. Thus, the 0.1*g* acceleration sustained at ground level can result in up to 0.3*g* on the upper floors of a building. In regions of low and moderate seismicity, furniture items and building contents are typically not restrained to the floor, or wall, of the building. Consequently, objects with aspect ratio greater than 3.3 (reciprocal of 0.3) are highly susceptible to overturning motions.

Once overturning motion commences, the unrestrained object may experience large out-of-plane displacement. Importantly, an object will not overturn provided the centre of gravity of the object has not been displaced beyond the limit for overturning [10]. Consequently, the seismic performance of unrestrained objects is critically dependent on the displacement demand behaviour of the building floor [11].

The overturning behaviour of free-standing objects has been studied for over a century. Early work including that of Milne published in 1885 [12] was based mainly on considerations of statical equilibrium and did not take into account the dynamic nature of the overturning actions [13]. A classical model for dynamic overturning, developed by Housner [14], provides estimates for the change in angular momentum of the object when one of its edges impacts with the ground in an overturning motion. The model is based on the assumptions that: (i) the impact action is perfectly inelastic meaning that there is no vertical motion of the edge while in contact with the ground following the impact, and (ii) the object experiences no deformation.

The classical model of Housner was found to be in good agreement with results obtained from dynamic experimentation of objects with aspect ratios of between 4 and 5 [15]. However, experimentation with squat objects (aspect ratio of 2) showed significant shortcomings of the model [16]. In subsequent studies (e.g. [17]), the classical model was modified based on calibrations with experimental data.

An elaborate theoretical model for dynamic overturning has been developed by Ishiyama [18,19], but the theoretical development has not been accompanied by adequate experimental verifications. In an alternative model developed by Lipscombe and co-workers [20,21], the classical expression for the change in angular momentum has been elegantly

extended to incorporate the "coefficient of restitution" (e) as a new term in the expression. If e equals zero, the modified expression is equivalent to the original classical expression assuming inelastic behaviour on impact. With the value of e varying between 0 and 1.0, the modified expression is able to take into account a range of conditions affecting the impact behaviour of the object. Importantly, the Lipscombe model has been verified experimentally. An important finding in the study is that the classical model for dynamic overturning will represent real behaviour reasonably accurately, provided that the object aspect ratio and the value of e fall within certain limits. For example, the classical model may be used if aspect ratio > 3 and $e \leq 0.7$. It is considered that slender objects at risk from overturning in a building (the subject of interest in this study) generally have their parameters falling within these limits.

The dynamic overturning behaviour of slender objects has been approximated by the analyses of elastic single-degree-of-freedom systems (refer Section 5 for further descriptions on linearization). The use of the elastic displacement floor spectrum in modelling the overturning of slender objects was introduced recently by Al Abadi et al [22], in which floor spectra obtained from the dynamic analyses of realistic models of actual multi-storey buildings in Melbourne and Singapore were reported.

According to floor amplification clauses in codes of practice, the filtering effects of the building amplify ground motions up its height. However, intuitively, the building may also behave as an isolation medium that attenuates the transmitted motions. These two perceptions seem contradictory. This paper, which represents a continuation of the study by Al Abadi et al [22], aims to resolve this significant dilemma and hence contribute to improving the fundamental understanding of the dynamical processes of damage to building contents.

The investigation described herein forms part of the long-term research strategy of the authors in addressing the potential impact of mild and moderate earthquake ground shaking on communities unprepared for earthquakes. The performance of non-structural components and building contents is of particular relevance in such earthquake scenarios. This is distinct from mainstream earthquake engineering research, which is mainly focused on the survival of structures under the ultimate conditions of severe earthquake ground shaking. This study was initiated by the perceived potential high consequences in cities such as Singapore, Bangkok and Hong Kong, which are characterised by high-rise and congested living environments. All three cities have a low level of preparedness for earthquakes and yet are subject to the threat of potential large magnitude long distance earthquakes which affect tall buildings in particular (e.g. [23-26]). Obviously, the findings from this study are generally applicable to other cities around the world experiencing similar conditions.

It is assumed in this study that the horizontal motions have been amplified much more than the vertical motions on a flexible site in a large magnitude distant earthquake (which could excite tall building structures into motion). Consequently, the effects of vertical ground excitations have not been taken into account.

Following a brief description of the building models (Sec. 2) and earthquake accelerograms (in Sec. 3) used in the study, seismic actions on the floor have been presented initially in terms of the acceleration demand (Sec. 4). The concept of floor displacement demand and the floor displacement spectrum, as first introduced in Al Abadi et al [22], has been briefly described for completeness in Sec. 5. Trends showing the filtering effects on the floor displacement demand of buildings having varying natural periods have been presented and discussed in Sec. 6. An explanation of the observed phenomena has been given in Sec. 7 to resolve the dilemma described above. Results of analyses involving numerous accelerograms recorded from past earthquake events have been compared in Sec. 8, in order to show the effects of the frequency content of the earthquake on the floor displacement demand behaviour. Results presented in Sections 6-8 constitute the principal original contributions to knowledge in this paper. Detailed recommendations for incorporation into building safety regulations cannot be made at this stage, as further research studies are warranted. There is a brief discussion at the end of the paper (Sec. 9) on future research directions and practical implementation of safety measures to mitigate seismic risk in buildings.

2. Building Models

The height of buildings considered in this study ranges between 50m and 280m. The corresponding fundamental natural period varies between 0.5 and 5.4 seconds. Reinforced concrete (RC) core walls constitute the main lateral load resisting elements of the buildings. These core walls are typically combined

with *RC* shear walls, or *RC*/steel moment frames to form the complete building system. The dynamic properties of each of the building systems may be represented by their natural period and mode shapes for the significant modes of vibration. These quantities were obtained for the Republic Plaza and Condominium buildings in Singapore based on ambient vibration measurements in the field (results were obtained for the first three significant vibration modes based on two-dimensional behaviour). The dynamic properties of the remaining three considered buildings (Harmony Block, Swire Building and TT Tsui Building in Hong Kong) were obtained from analyses of finite element models, calibrated against the natural periods of vibration obtained from field monitoring of ambient vibration. Thus, the dynamic properties obtained for each building were based, at least partly, on measurements and not wholly on computer modelling.

Results for the translational modes of vibration in the two orthogonal directions have been presented separately, whilst torsional vibration has been ignored. Both the natural periods and mode shapes are fairly similar in the two directions. Table (1) presents a "summary at a glance" of the basic information related to the buildings considered in this study.

Basic information on each building, including typical floor plans and their respective mode shapes, are contained in the literature references cited in Table (1). The buildings are classified into three categories according to the building height and fundamental natural period, as shown in the first column of Table (1).

It is established in this paper (Sec. 7) that the natural period of the building and its relation to the ground dominant period of excitation define the distribution of floor hazard along the height of the building. In other words, each building category has its own distinct hazard distribution pattern for a given earthquake scenario. However, comparison of the mode shapes reveals no major difference between the building categories, see Figure (2).

Table 1. Information summary for buildings considered.

Category	Building	Height (m)	Construction Form	Natural Periods of 1st and 2nd Modes (sec)	Ref's.
A	Republic Plaza	280	Core Walls and Steel Frames	1st : 5.4 2nd : 1.5	[27]
B	Condominium	90	Core Walls and RC Frames	1st : 1.5 2nd : 0.4 3rd : 0.2	[27]
B	Harmony Block	115	Core Walls and Shear Walls	1st: 0.7–0.8 2nd: 0.35 –0.4	[28]
C	Swire Building	51	Core Walls and RC Frames	1st: 0.55–0.60 2nd: 0.18 – 0.2	[28]
C	TT Tsui Building	51	Core Walls and RC Frames	1st: 0.55–0.60 2nd : 0.15-0.16	[28]

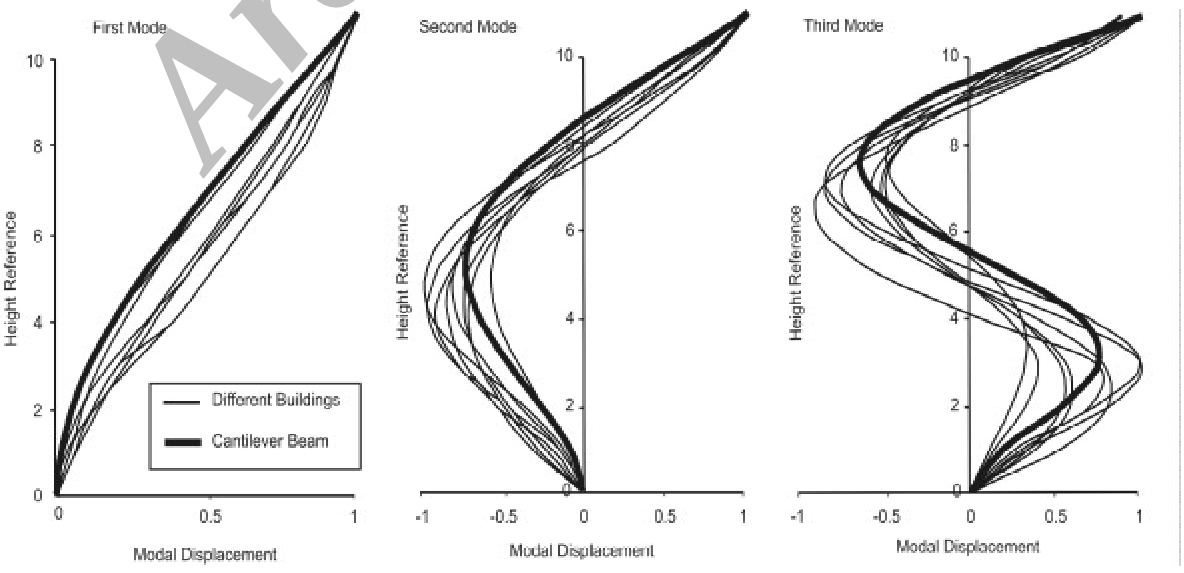

Figure 2. Mode shapes for all considered buildings.

3. Earthquake Accelerograms

This study is based mainly on large magnitude earthquake scenarios, because the response of tall buildings would be insensitive to small magnitude earthquakes possessing high frequency contents. Most of the analyses employed an ensemble of computer simulated accelerograms for a sizeable $M = 7$ earthquake with a generous source-site distance of $90km$ (i.e. $M = 7$ $R = 90km$), in order that the amplitude of the excitation is consistent with the damage scenario of a moderate earthquake. The average peak ground acceleration of the simulated accelerograms is in the order of $0.05g$ and the peak ground velocity is typically around $70mm/sec$, which corresponds to Intensity VI-VII shaking on the Modified Mercalli Intensity scale. Bedrock accelerograms were first simulated for generic rock conditions using computer program GENQKE [29]. One-dimensional filters were then applied to modify the accelerograms for average "Class C" (shallow soil) site conditions, as defined by the new Australian Standard for earthquake actions (Draft [5]). Further analyses have been undertaken using accelerograms recorded from large magnitude far-field earthquakes (see Table (2) for the complete listing).

Table 2. Accelerograms employed for analys[es].

Type of Accelerogram	Magnitude (M)	Distance (km)	Location and Co[untry]	[Date] of Event
Computer Simulations [29]	7.0	90 km	[N]A.	N.A.
Recorded	8.1	[4]km	[Mex]ico City, Mexico	May 1985
Recorded	7.8	400 k[m]	Si[n]gapore	June 2000
Recorded	7.9	290 km	Honshu, Japan	May 1968
Recorded	7.9	[2]km	Panguna, Papua New Guinea	July 1971

* parameters used [in] the simulations have been calibrated against recorded accelero[grams] at 700 km epicentral distance [24].

4. Floor Acceleration Demand

A comparison of the floor acceleration spectra for the Condominium (Category 2) building subjected to a $M = 7$ $R = 90km$ earthquake scenario reveals peak floor acceleration (PFA) at the roof level of the building to be almost double of that at mid-height and ground levels. Note, PFA is only representative of the acceleration of rigid objects with perfect attachment to the floor supports. Significant shifts in the object natural period could occur following loosening of the support. Thus, the highest point on the response spectrum, defined herein as RSA_{max}, can be taken as an acceleration parameter representing the hazard level of the floor, see Figure (3).

The height-wise distribution of the above acceleration demand parameter is shown in Figure (4). The distribution trend shown in this figure is considerably different to the linear function stipulated by current earthquake codes of practice (see straight-line in Figure (5)).

Results obtained for all the buildings considered in this study are compared in Figure (5). The comparison shows similar trends for the Category A

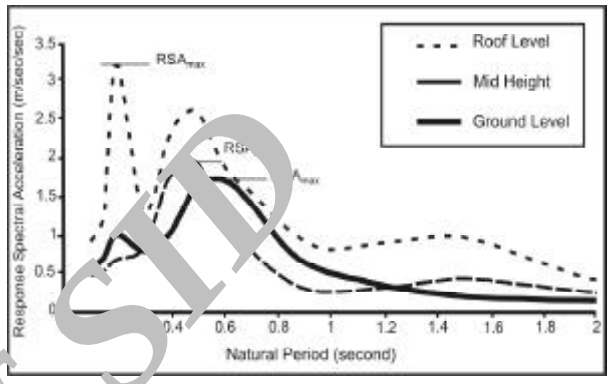

Figure 3. Acceleration floor spectra for condominium (Category B) building.

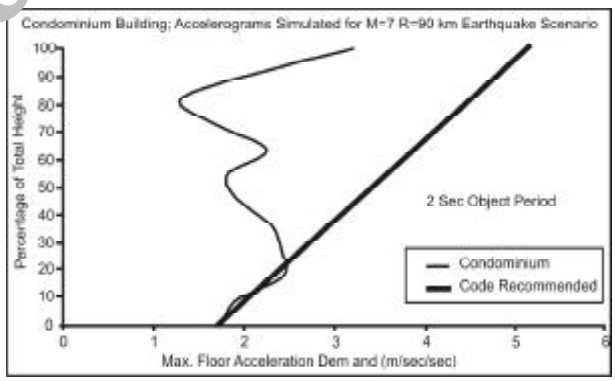

Figure 4. Vertical distribution of floor acceleration demand for condominium (Category B) building.

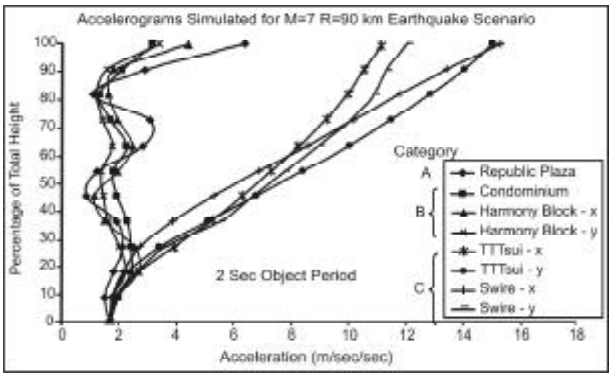

Figure 5. Vertical distribution of floor acceleration demand for all considered buildings.

and B buildings. However, the trends for Category C (low-rise) buildings are in reasonable agreement with code recommendations (e.g. Draft [5]). The large differences in the floor acceleration demand behaviour between the building categories have been highlighted by the comparison. These important differences have not been reflected by provisions in most existing building standards.

As previously discussed, neither of the acceleration parameters (*PFA* and RSA_{max}) are directly indicative of the overturning behaviour of objects. The anomalies revealed in this section call for further investigation into seismic actions in high-rise buildings, with direct reference to displacement behaviour.

5. Displacement Representation of Overturning

Using the substitute-structure method, the maximum out-of-plane displacement developed in a slender object experiencing rocking behaviour can be approximated by the analysis of an idealised elastic single-degree-of-freedom (*SDOF*) system possessing effective stiffnesses (K_{eff}) and hence effective natural period (T_{eff}), as shown in Figure (6a). The object considered is assumed to be rigid and free-standing. Thus, the base-shear versus effective displacement relationship features: (i) a vertical line at zero displacement and (ii) a straight-line representing the linear decrease in resistance to overturning with increasing displacement. This force-displacement behaviour is the result of geometrical non-linearity (also known as "P-delta" effects).

The natural period of rocking motion is non-unique and is amplitude dependent (i.e. period shifts with time in a non-stationary response). The estimated displacement demand is taken as the highest point on the displacement spectrum between the "initial" and the "shifted" period (see Figure (6b) for a schematic

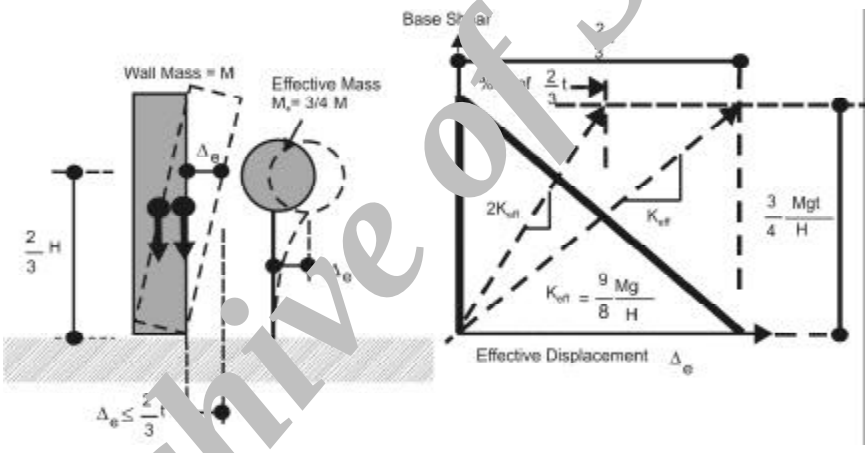

Effective Period (100% disp) $T_{eff} = 2\pi\sqrt{\frac{M_e}{2k_{eff}}} = 2\pi\sqrt{\frac{\frac{3}{4}M}{\frac{9}{8}\frac{Mg}{H}}} = 2\pi\sqrt{\frac{2}{3}\frac{H}{g}}$ *Effective Period (50% disp)* $T_{eff} = 2\pi\sqrt{\frac{M_e}{2k_{eff}}} = 2\pi\sqrt{\frac{\frac{3}{4}M}{\frac{9}{4}\frac{Mg}{H}}} = 2\pi\sqrt{\frac{H}{3g}}$

Figure 6a. Substitute-structure model for the linearisation of rocking motion.

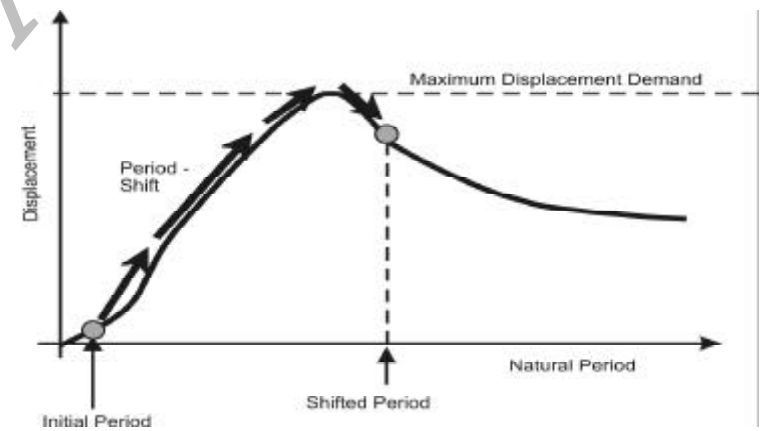

Figure 6b. Use of elastic displacement spectrum in estimating object displacement.

representation). The "initial" period may be taken as "zero", or very close to zero, given that objects can be assumed to be rigid up to the commencement of overturning. The "shifted" period at the threshold of overturning (i.e. at "full" amplitude) may be estimated using Eq. (1a) based on the linearization described in Figure (6a).

$$T = 2\pi\sqrt{(2H/3g)} \qquad (1a)$$

The highest point on the displacement spectrum, which defines the displacement demand on the object, does not necessarily appear as a prominent peak when plotted in the conventional acceleration response spectrum format. Thus, the approach of tracking the maximum displacement demand from a displacement spectrum would not have been possible using an acceleration spectrum.

The object is considered to have overturned if the estimated displacement demand exceeds two-thirds of the width of the object, see Figure (6a). More detailed description of the linearization approach and the use of the floor displacement spectrum in predicting overturning of objects have been given in Al Abadi et al [22].

This simplified method of using an elastic displacement spectrum based on 5% critical damping to predict the displacement demand of a rocking object (which was developed initially from research on the out-of-plane behaviour of unreinforced masonry walls) is supported by time-history analyses in conjunction with shaking-table tests [30,31]. However, it is noted that substitute-structure modelling is only meant to provide an approximation to the actual responses. Nevertheless, such an approach serves the needs of this study.

In view of errors associated with the linearization of a rocking response, it is prudent to limit the object displacement to 50% of its theoretical limit for overturning. Thus, an object is considered to be subject to high overturning risk if the estimated displacement demand exceeds one-third of the width of the object (i.e. half of two-thirds). Note, the "shifted" period depends on the displacement amplitude. Accordingly, it is recommended that Eq.1b be used in place of Eq.1a in calculating the effective natural period of a slender object as shown in Figure 6a.

$$T = 2\pi\sqrt{(H/3g)} \qquad (1b)$$

The direct correlation defined by Eqs. (1a) and (1b) between the "shifted" period (T) and the object height is shown in Table (3). It is noted that for slender objects the effective period for rocking is controlled only by its height and not its width or aspect ratio.

Table 3. Shifted periods for slender rectangular objects.

Object Height (m)	Shifted Period Eq.1a (sec)	Shifted Period Eq.1b (sec)
0.50	1.2	0.8
0.75	1.4	1.0
1.00	1.6	1.2
1.50	2.0	1.4
2.00	2.3	1.6
3.00	2.8	2.0

Results related to floor displacement demand, as presented in the remainder of the paper, have been based on objects having 1 and 2 sec periods, and with a notional 5% critical damping to emulate energy loss experienced during rocking. These periods correspond to object heights of 0.75m and 3m, respectively, based on Eq. (1b) (which represents conditions of objects experiencing displacement of up to 50% of their theoretical limit for overturning).

Vertical Distribution of Floor Displacement Demand

The displacement floor spectra at roof, mid-height and ground levels show a gradual, and uniform, increase of the displacement demand for a Category C (e.g. TT Tsui) building along its height, as shown in Figure (7). Clearly, the filtering actions of the building have amplified the seismic waves and by a factor of up to 5 (from 0.02m displacement to 0.1m displacement) at a period of 0.6 sec, which is close to the natural period of the building. According to the failure criterion defined in Sec. 5, objects located at the upper levels of the building, with width not exceeding 300mm (3 times 0.1m) and height of over half a metre (period exceeding 0.8 sec according to Table (3)), are at risk of overturning.

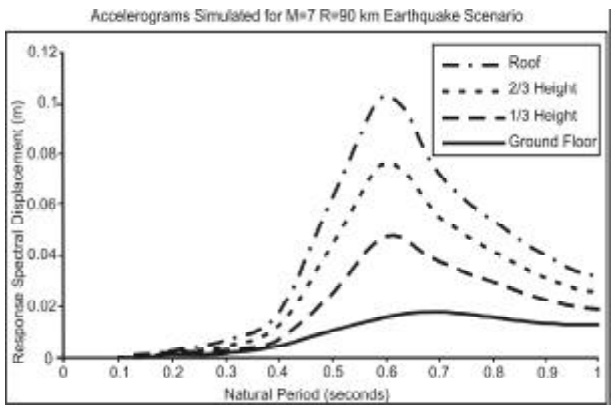

Figure 7. Displacement floor spectra for TT Tsui (Category C) building.

Displacement floor spectra presented for the Category B (Condominium) building, as shown in Figure (8), are in interesting contrast to those presented for Category C buildings, when both are subjected to the same earthquake. For the Category B (Condominium) building, the response spectra of the building floors at both the mid-height and roof levels show peaks occurring at natural periods of around 0.5 and 1.5 sec. These are, respectively, the natural periods of the 1st and 2nd modes of vibration of the analysed building. Importantly, the amplitudes of these peaks are highly suppressed, in comparison with those shown in Figure (7). There is no significant amplification at the first peak (at 0.5 sec). Furthermore, displacement demand in the period range of 0.5-1.2 sec in the mid-height region of the building is shown to be attenuated. The filtering actions of the building seem to have an isolation effect on the building contents. The highest displacement demand at roof level is estimated at 60*mm* (in comparison with 100*mm*) and at a natural period of 1.5 sec. According to the failure criteria defined in Section 5, very slender objects with depth of 180 mm (3 times of 60*mm*) and height exceeding 1.5*m* (see Table (3)) are marginally at risk of overturning.

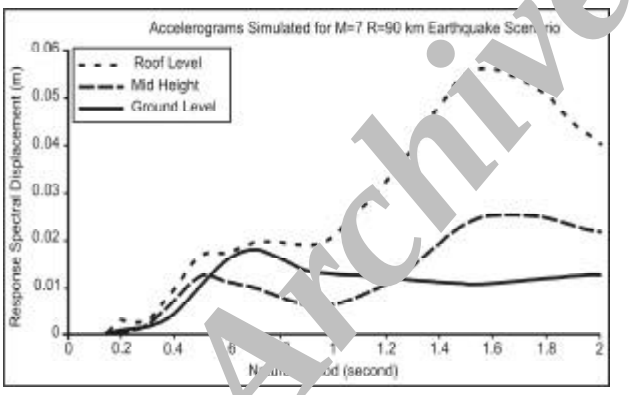

Figure 8. Displacement floor spectra for condominium (Category C) building.

Further comparisons of the vertical distribution of the floor seismic displacement demands have been made, see Figure (9), including all buildings considered in this study. The displacement demands shown in this figure were based on an effective natural period of 2 sec. Each point on the displacement demand chart in Figure (9) is based on the highest point on the respective floor displacement spectrum for natural periods up to 2 sec. It is shown that for most Category A and Category B buildings,

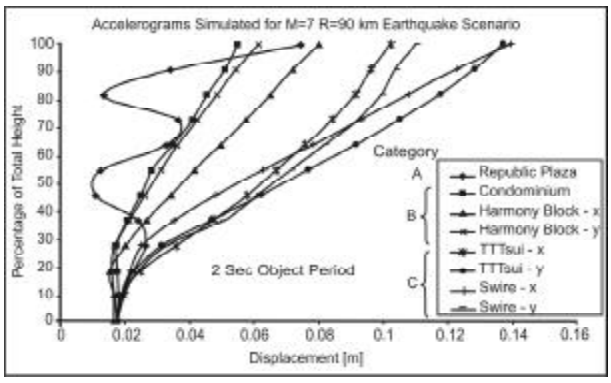

Figure 9. Vertical distribution of floor displacement demand for all considered buildings.

the floor displacement demand increases by some 10-20*mm* from ground to mid-height level; and by a further 20-30*mm* from mid-height to roof level. In comparison, the seismic displacement demand for Category C building increases, on average, by some 40*mm* from ground to mid-height level, and by a further 60*mm* from mid-height to roof level.

It is shown in the above comparison that the seismic displacement demand of floors in high-rise (Category A and B) buildings is overall significantly lower than that in medium and low-rise (Category C) buildings. Thus, the displacement demand behaviour of building floor contents (which decreases with increasing building height) is in interesting contrast to that of the lateral deflection of the building itself (which increases with increasing building height).

This phenomenon is depicted schematically in Figure (10), which shows that objects located at a common elevation of, say, 50*m* would be displaced by

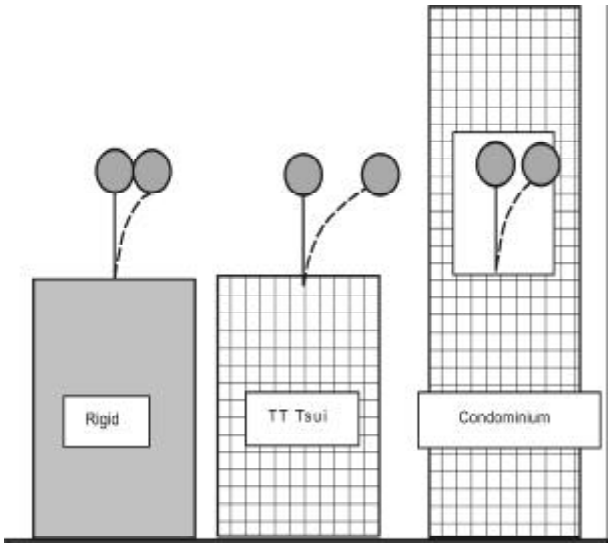

Figure 10. Reduction in floor displacement demand by isolation effects in tall buildings.

a considerably smaller extent in a 100*m* high building (at mid-height level) than in a 50*m* high building (at roof level). Furthermore, the distribution patterns of the floor displacement demand between these building categories are also very different.

The floor spectra presented in this section demonstrate both amplification and isolation actions of the building in terms of their effects on the overturning of objects. Their occurrences are highly dependent on the building properties, since both phenomena were found from analyses of response to the same earthquake. It is inferred from the limited analysis results that attenuation action is likely if the fundamental natural period of vibration of the building significantly exceeds the dominant period of the ground excitations. Explanation for their cause has been discussed in detail in Section 7.

7. Isolation Actions in High-Rise Buildings and Explanation of the Cause

The effects of the filtering actions of buildings have been further investigated by inputting a simulated ground motion to the linear filter of a single-degree-of-freedom (*SDOF*) system with natural periods of 1.5 sec and 0.5 sec (which correspond, respectively, to the fundamental natural periods of Category B and C buildings, as considered in Section 6). The input and filtered displacement time-histories (which represent, respectively, the ground and floor motions) are presented in Figures (11a) and (11b) in a time window of 6 sec duration.

Figure (11a) shows such a time window for the 0.5 sec filter. The amplitude of the filtered motion is some 2-4 times that of the input motion. Note that the displacement response of the object on the building floor is the sum of the effects of the ground (input) displacement and the relative displacement of the building floor. Significantly, the two motions pertain to be in-phase, implying that major peaks of the two motions occur at around the same instances (e.g. at 4 sec). The effects of the two motions are therefore additive. A similar analysis was conducted on the 1.5 sec filter. Figure (11b) shows that the input and filtered motions are generally out-of-phase. Thus, the effects of the two motions are partially self-cancelling.

Observations from such analyses contribute to the understanding of the reason for floor displacement amplification in the 0.5 sec building, and attenuation in the 1.5 sec building, as described in Section 6. These observations arising from the analyses are consistent with well-known basic principles of dynamics in that a linear filter subject to sinusoidal input excitations will experience in-phase, or out-of-phase, responses depending on the period of the input excitations in relation to that of the linear filter.

The filtered motions presented in Figures (11a) and (11b) were based on the response of *SDOF* systems. The filtering effect of a *MDOF* system can be represented by the weighted sum of one or more of such (*SDOF*) filters, each of which corresponds to a significant mode of vibration in the *MDOF* system. The motion associated with each *SDOF*

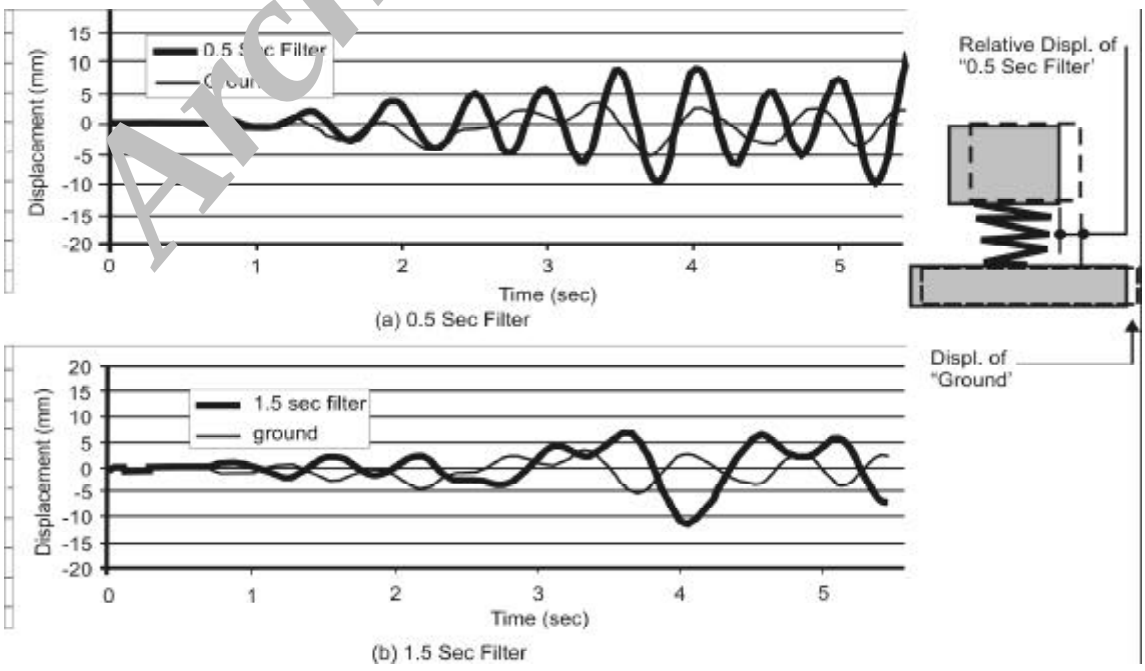

Figure 11. Displacement time-history of filtered motions.

filter is scaled by the respective mode shape factor and participation factor. Such multi-modal effects have been incorporated, as described, into the computation of the floor motions. The response displacement time window of a 1 sec object when excited by the computed floor motion at mid-height level of the Condominium building is shown in Figure (12a). It is shown that the response to the ground motion partially offsets the response to the floor motion (as represented by the *MDOF* filter). This cancellation phenomenon is consistent with the behaviour of the *SDOF* filter, as described above.

However, interestingly, the filtering effects of the floor have not attenuated the displacement response of the 2 sec object (in the same way as they attenuated the 1 sec object), as shown by the time-window of Figure (12b). It is shown by comparing Figure (12a) with Figure (12b) that the attenuation effects of the building are selective, and are dependent on the natural period of the object. This is further exemplified in Figure (13), which compares the displacement demand distribution of a 1 sec and 2 sec object along the height of the Condominium building. The noticeable attenuation at mid-height level reflects the

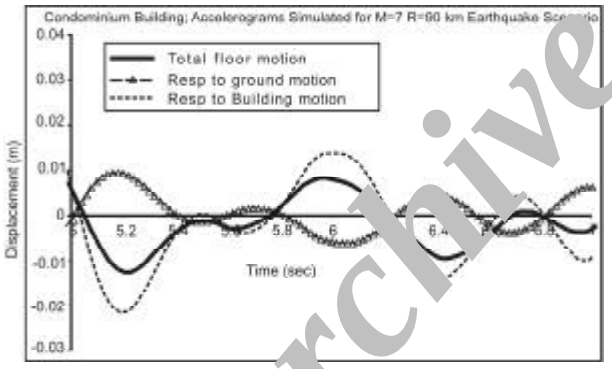

Figure 12a. Response time-history for 1 sec object at mid-height level in condominium building.

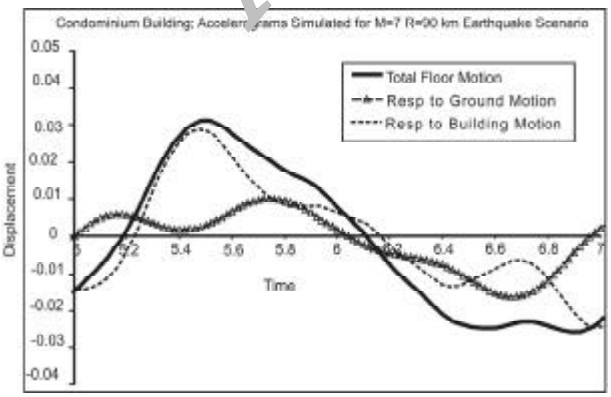

Figure 12b. Response time-history for 2 sec object at roof level in condominium building.

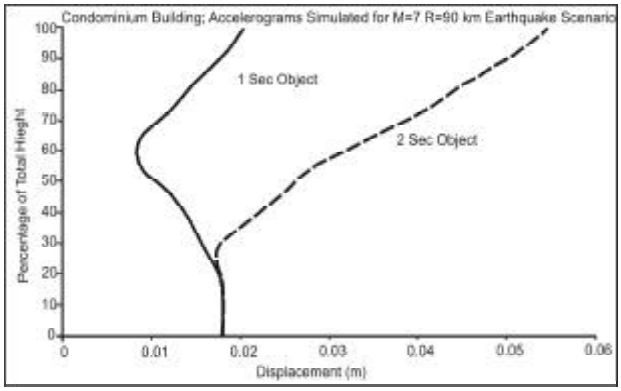

Figure 13. Vertical distribution of floor displacement demand for 1 and 2 sec object floor.

contribution of the 2nd mode of vibration to the selective attenuation actions.

8. Influence of Ground Motion Response Spectrum Properties

Dynamic analysis results, as presented above, were based on computer simulated accelerograms consistent with the $M = 7$ $R = 90km$ earthquake scenario event. Further analyses have been undertaken using numerous recorded accelerograms (refer Section 3), including that recorded on rock outcrop in the far-field during the 1985 Mexican earthquake. The displacement response spectra associated with each ground motion records employed in this study have been shown in Figure (14).

The vertical distribution of the floor displacement demand associated with the Mexican earthquake accelerograms is presented in Figure (15), for comparison with Figure (9). The two figures have commonality in terms of showing distinctly different distribution patterns between high-rise and medium-rise buildings. An important difference associated with the various accelerograms is the relative

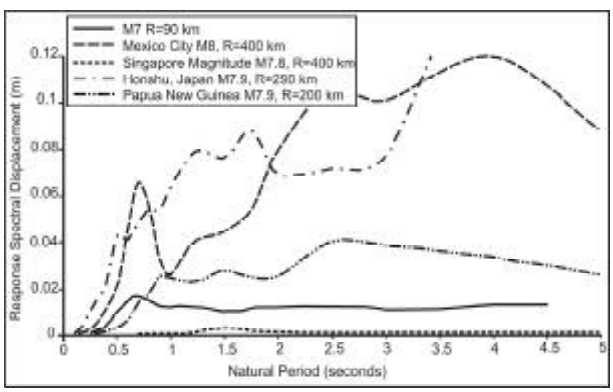

Figure 14. Displacement ground spectra for all accelerograms employed in analyses.

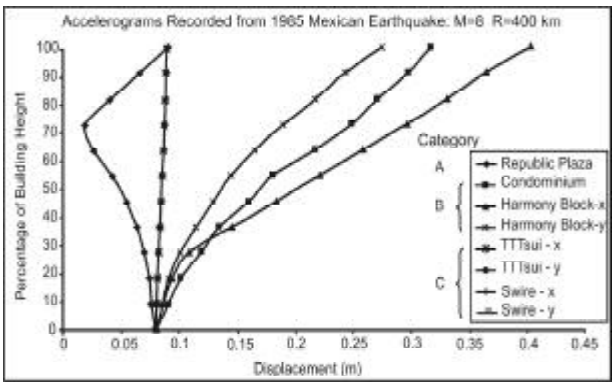

Figure 15. Vertical distribution of floor displacement demand for all considered buildings.

magnitude of the floor displacement demand between Category B and C buildings. It is noted that the first corner period of the accelerogram recorded at Mexico City is at around 1.5 seconds, see Figure (14). This is close to the fundamental period of vibration of the Category B buildings and to the period of the second mode of vibration in Category A buildings. Consequently, the Mexican earthquake excitations induce some resonant effects in Category B buildings whilst displaying very pronounced isolation effects at mid-height level in a Category A building.

Further comparison of the distribution patterns of floor displacement demand is shown in Figure (16), for the Condominium (Category B) buildings. Results associated with both the computer simulated accelerograms (M=7 R=90 km) and the accelerograms recorded at Panguna display most significant isolation effects. It is important to note that the first corner period of both accelerograms is at around 0.5-0.6 sec, which is in proximity to the natural period of the second mode of vibration of the building (0.43 sec).

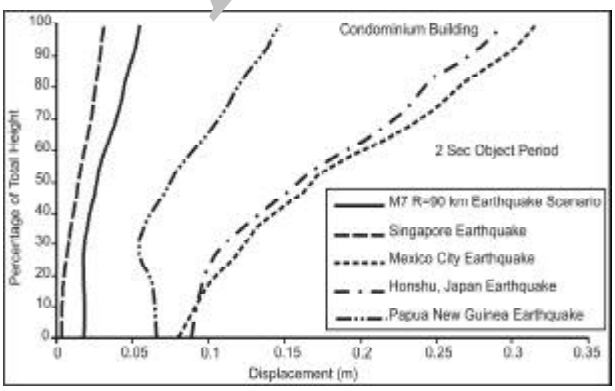

Figure 16. Vertical distribution of floor displacement demand for condominium buildings.

9. Practical Considerations and Further Research

This paper is an initial contribution to achieving the long-term objective of incorporating effective regulatory control in a multi-storey building for mitigating potential seismic risks to its contents, particularly free-standing objects. The most effective approach of mitigating overturning risks is, in theory, to provide adequate restraints (e.g. by straps and brackets) to every individual object and component that appears at risk. However, such seismic mitigation measures, whilst carried out with good intentions, can be impractical and very intrusive, and often meet with resistance. This is particularly the case in areas that have not been subjected to frequent earthquake activities. In view of this, the recommended approach is to accurately identify objects that are truly at risk, in order to correctly focus attention. Some suggestions are made herein based on results presented in the paper. However, detailed recommendations cannot be formulated as further research is required to incorporate a more diverse range of building models into parametric studies.

According to the conventional force-based design criterion, unrestrained objects with aspect ratios exceeding 3-4 are deemed to be at risk from overturning, even in conditions of moderate seismicity. The alternative displacement-based approach, that characterizes overturning risks in terms of the object height and base dimensions, provides a more accurate evaluation. The use of object height and base dimensions as separate criteria to ascertain overturning risk is potentially easier to understand, and to implement, in routine inspections of building facilities. For example, storage racks containing hazardous materials, or with constant exposure to occupants, should be subject to restrictions in height, except when base-dimension and/or base restraints requirements are fulfilled.

The natural period of a building in relation to that of the site has also been identified in the paper to be a key factor controlling the overturning behaviour of its contents. Importantly, it is clear from results presented that the level of hazard does not increase indefinitely with increasing building period. It is hypothesized at this stage (subject to confirmation by further investigations) that the maximum floor displacement demand in the building increases with its natural period, up to the critical limit at which point the building period is comparable to the site period. The displacement demand will decrease with further

increase in the natural period of the building. When the correlation of the floor displacement demand with the building period is fully established and validated, individual buildings could be rated readily for their seismic risk level. It is important, however, to represent the natural period of the building by easy-to-measure parameters such as height of building, or number of storeys (despite that accuracy may thereby be compromised since two buildings with the same number of storeys will not have identical natural periods). Meanwhile, high hazard areas (identified with high site period) could be identified for the purpose of prioritising regulatory control.

10. Conclusions

- This paper highlights the need to control the disposition and restraints of building contents in multi-storey buildings in cities with low level of preparedness for potential earthquake hazards as one of the key considerations for workplace safety.
- The risk of an object overturning can be estimated from the dual independent criteria of its width and height, as opposed to the usual single criterion of the object aspect ratio (or slenderness ratio) based on static analysis. An object is at risk from overturning if its width is exceeded by one-third of the displacement demand as determined from the elastic displacement response spectrum of the building floor. The equivalent object period is correlated directly with its height according to the substitute-structure model. For example, 1 sec and 2 sec objects have heights of 0.75m and 3m, respectively.
- The filtering effects of the Category B building have been shown to attenuate the displacement demand on objects, which is in interesting contrast to the Category C building, which amplifies the object displacement demand. Floor spectra of the buildings demonstrated both amplification and isolation actions. Their occurrences depend strongly on the building properties, since both phenomena were found from analyses of the same earthquake. It is inferred from the limited analysis results that attenuation action is likely if the fundamental natural period of vibration of the building significantly exceeds the dominant period of the ground excitations.
- Inspections of the displacement time-histories revealed that phase match between the ground displacement and the floor displacement time-histories dictates if the motion is amplified, or attenuated by the filtering effects of the building.
- The response of a 1 sec (0.75m high) object is predicted to be much more sensitive to the attenuation actions than a 2 sec (3m high) object, when subject to ground excitations of a $M = 7$ $R = 90km$ earthquake scenario. Significantly, the attenuation action is selective, as exemplified by the comparison of the displacement demand profiles associated with objects having different height ranges.
- The floor displacement attenuation/amplification behaviour of the building is dependent on the frequency content of the ground excitations. Thus, the displacement demand profile in the building could change significantly with earthquake scenarios characterised by different frequency contents.
- Preliminary recommendations have been made in implementing seismic risk mitigating measures that involve rating individual buildings and routine inspections of their contents. The check for compliance could be based on object height and base dimensions as separate criteria.

Acknowledgements

The financial and academic support from University of Munich, Germany, in organising and funding the 5-month visit of the first author to University of Melbourne in 2003-2004 is gratefully acknowledged. Assistance provided by post-graduate research student Haider Al Abadi from The University of Melbourne and Neaz Sheikh from The University of Hong Kong during the visit of the first author to Melbourne is also acknowledged. The research findings reported in this paper forms part of the Hong Kong-Melbourne collaborative research project entitled "Seismic Vulnerability Models for Non-Structural Components in Buildings". The project is being funded by the Hong Kong Research Grant Council for 2003-2006.

References

1. Rodriguez, M.E., Restrepo, J.I., and Carr, A.J. (2002). “Earthquake-Induced Floor Horizontal Accelerations in Buildings”, *Earthquake Engineering and Structural Dynamics*, **31**(3), 693-718.

2. Naeim, F. (1999). “Lessons Learned from

Performance of Nonstructural Components during the January 17, 1994 Northridge Earthquake - Case Studies of Six Instrumented Multistory Buildings", *Journal of Seismology and Earthquake Engineering*, **2**(1), 47-57.

3. FEMA 273/274 (1997). NEHRP Guidelines for the Seismic Rehabilitation of Building, Report FEMA 273 (Guidelines), FEMA 274 (commentary), Federal Emergency Management Agency, Washington DC, USA.

4. IBC (2003). International Code Council. International Building Code, 2003. U.S.A.

5. AS1170.4 (1993). Standards Association of Australia: "Minimum Design Loads on Structures: Part 4: Earthquake Loads - AS1170.4 and Commentary".

6. Draft AS/NZS 1170.4 (2004). Draft for Public Comment Australian Standard for Structural Design Actions, Part 4: Earthquake Actions in Australia. Document No. DR 04303.

7. NZS 4203 (1992). Standard New Zealand: Code of Practice for General Structural Design and Design Loading for Buildings.

8. Tillander, K. (2004). "Utilisation of Statistics to Assess Fire Risks in Building, Dissertation for the Degree of Doctor of Science in Technology", Department of Civil and Environmental Engineering, Helsinki University of Technology, Finland. VTT publication no. 537. Accessed by the authors from the following website : http://www.vtt.fi/inf/pdf/publications/2004/P537.pdf.

9. Lam, N.T.K., Wilson, J.L., Doherty, K., and Griffith M. (1998). "Horizontal Seismic Forces on Rigid Components within Multi-Storey Buildings", *Proceedings of the Australasian Structural Engineering Conference*, Auckland (Ed. Butterworth), Published by Structural Engineering Society of New Zealand, 721-726.

10. Lam, N.T.K. and Wilson, J.L. (2001). "The Seismic Assessment of Building Parts and Contents: A Displacement Based Approach", *Proceedings of the Annual Technical Conference for the New Zealand National Society for Earthquake Engineering (NZNSEE)*, Wairakei, New Zealand, Published by NZNSEE. Paper no.5.01.

11. Lam, N.T.K. and Gad, E. (2002). "An Innovative Approach to the Seismic Assessment of Non-Structural Components in Buildings", *Procs. of the Australian Earthquake Engineering Society (AEES) Annual Seminar*, Adelaide, (Ed. Griffith et al). Published by AEES. Paper no.10.

12. Milne, J. (1885). "Seismic Experiments", Transactions of the Seismic Society of Japan, **8**, 1-82.

13. Yim, C.S., Chopra, A.K., and Penzien, J. (1980). "Rocking Response of Rigid Blocks to Earthquakes", *Earthquake Engineering and Structural Dynamics*, **8**, 565-587.

14. Housner, G.W. (1963). "The Behaviour of Inverted Pendulum Structures", *Bulletin of the Seismological Society of America*, **53**(2). 403-417.

15. Aslam M., Godden, W.G., and Scalise, D.T. (1980). "Earthquake Rocking Response of Rigid Bodies", *Journal of the Structural Division, ASCE*. **106**, 377-392.

16. Priestley, M.J.N., Evison, R.J., and Carr A.J. (1978). "Seismic Response Analysis of Structure Free to Rock on Their Foundations", Bulletin of the New Zealand National Society for Earthquake Engineering, **11**(3), 141-150.

17. Spanos, P.D. and Koh, A.S. (1984). "Rocking of Slender Rigid Bodies Allowed to Uplift", *Earthquake Engineering and Structural Dynamics*, **11**, 57-76.

18. Ishiyama, Y. (1980). "Review and Discussion on Overturning of Bodies by Earthquake Motions", Paper No. 85, Building Research Institute, Japan.

19. Ishiyama, Y. (1982). "Motions of Rigid Bodies and Criteria for Overturning by Earthquake Excitations", *Earthquake Engineering and Structural Dynamics*, **10**, 635-650.

20. Lipscombe, P.R. and Pellegrino, S. (1989). "Rocking of Rigid-Block Systems under Dynamic Loads", Applied Solid Mechanics 3 (ed. Allison I.M. and Ruiz C.), Elsevier Applied Science, 175-189.

21. Lipscombe, P.R. (1990). Dynamics of Rigid Block Structures, Dissertation Submitted to the University of Cambridge for the degree of Doctor of Philosophy.

22. Al Abadi, H., Lam, N.T.K., Gad, E., and Chandler, A.M. (2004). "Earthquake Floor Spectra for Unrestrained Building Components", *International Journal of Structural Stability and Dynamics*, **4**(3), 361-377.

23. Warnitchai, P. and Sangarayakul, C. (2000). "Seismic Hazard in Bangkok due to Distant Earthquakes", *Procs. of the 2nd Multi-lateral Workshop on Development of Earthquake and Tsunami Disaster Mitigation Technologies and their Integration for the Asia-Pacific Region*, 147-156.

24. Balendra, T., Lam, N.T.K., Wilson, J.L., and Kong K.H. (2002). "Analysis of Long-Distance Earthquake Tremors and Base Shear Demand for Buildings in Singapore", *Journal of Engineering Structures, 2002*; **2**, 99-108.

25. Lam, N.T.K., Wilson, J.L., Chandler, A.M., and Hutchinson, G.L. (2002). "Response Spectrum Predictions for Potential Near-Field and Far-Field Earthquakes Affecting Hong Kong: Rock Sites", *Soil Dynamics and Earthquake Engineering*, **22**, 47-72.

26. Chandler, A.M. and Lam, N.T.K. (2004). "An Attenuation Model for Distant Earthquakes", *Earthquake Engineering and Structural Dynamics*, **33**, 183-210.

27. Brownjohn, J.M.W. and Pan, T.C. (2001). "Response of Tall Buildings to Weak Long Distance Earthquakes", *Earthquake Engineering and Structural Dynamics*, **30**(5), 709-729.

28. Su, R.K.L., Chandler, A.M., Sheikh, M.N., and Lam, N.T.K. (2005). "Influence Of Non-Structural Components On Lateral Stiffness of Tall Buildings", *Journal of Structural Design of Tall Buildings*, In press.

29. Lam, N.T.K., Wilson, J.L., and Hutchinson, G.L. (2000). "Generation of Synthetic Earthquake Accelerograms Using Seismological Modeling: a Review", *Journal of Earthquake Engineering*; **4**(3), 321-354.

30. Doherty, K., Griffith, M., Lam, N.T.K., and Wilson, J.L. (2002). "Displacement-Based Analysis for Out-of-Plane Bending of Seismically Loaded Unreinforced Masonry Walls", *Earthquake Engineering and Structural Dynamics*, **31**(4), 833-850.

31. Lam, N.T.K., Griffith, M.C., Wilson, J.L., and Doherty, K. (2003). "Time-History Analysis of URM Walls in Out-of-Plane Flexure", *Journal of Engineering Structures*, **25**, 743-754.